

Proceeding Paper

# Molybdenum Disulfide Field Effect Transistors under Electron Beam Irradiation and External Electric Fields <sup>†</sup>

Aniello Pelella <sup>1,2</sup>, Alessandro Grillo <sup>1,2,\*</sup>, Enver Faella <sup>1</sup>, Filippo Giubileo <sup>2</sup>, Francesca Urban <sup>1,2</sup> and Antonio Di Bartolomeo <sup>1,2</sup>

<sup>1</sup> Physics Department “E. R. Caianiello”, University of Salerno, Via Giovanni Paolo II 132, Fisciano, 84084 Salerno, Italy; apelella@unisa.it (A.P.); efaella@unisa.it (E.F.); furban@unisa.it (F.U.); adibartolomeo@unisa.it (A.D.B.)

<sup>2</sup> CNR-SPIN Salerno Via Giovanni Paolo II 132, Fisciano, 84084 Salerno, Italy; filippo.giubileo@spin.cnr.it

\* Correspondence: agrillo@unisa.it

<sup>†</sup> Presented at the 2nd International Online-Conference on Nanomaterials, 15–30 November 2020; Available online: <https://iocn2020.sciforum.net/>. Published: 15 November 2020.

**Abstract:** In this work, monolayer molybdenum disulfide (MoS<sub>2</sub>) nanosheets, obtained via chemical vapor deposition onto SiO<sub>2</sub>/Si substrates, are exploited to fabricate field-effect transistors with n-type conduction, high on/off ratio, steep subthreshold slope and good mobility. We study their electric characteristics from 10<sup>-6</sup> Torr to atmospheric air pressure. We show that the threshold voltage of the transistor increases with the growing pressure. Moreover, Schottky metal contacts in monolayer molybdenum disulfide (MoS<sub>2</sub>) field-effect transistors (FETs) are investigated under electron beam irradiation conditions. It is shown that the exposure of Ti/Au source/drain electrodes to an electron beam reduces the contact resistance and improves the transistor performance. It is shown that e-beam irradiation lowers the Schottky barrier at the contacts due to thermally induced atom diffusion and interfacial reactions. The study demonstrates that electron beam irradiation can be effectively used for contact improvement though local annealing. It is also demonstrated that the application of an external field by a metallic nanotip induces a field emission current, which can be modulated by the voltage applied to the Si substrate back-gate. Such a finding, that we attribute to gate-bias lowering of the MoS<sub>2</sub> electron affinity, enables a new field-effect transistor based on field emission.

**Keywords:** electron beam; molybdenum disulfide; field emission; two-dimensional; field effect transistor

**Citation:** Pelella, A.; Grillo, A.; Faella, E.; Giubileo, F.; Urban, F.; Di Bartolomeo, A. Molybdenum Disulfide Field Effect Transistor under Electron Beam Irradiation and External Electric Field. *Mater. Proc.* **2021**, *4*, 25. <https://doi.org/10.3390/IOCN2020-07807>

Academic Editors: Ana María Díez-Pascual and Guanying Chen

Published: 10 November 2020

**Publisher’s Note:** MDPI stays neutral with regard to jurisdictional claims in published maps and institutional affiliations.



**Copyright:** © 2020 by the authors. Licensee MDPI, Basel, Switzerland. This article is an open access article distributed under the terms and conditions of the Creative Commons Attribution (CC BY) license (<http://creativecommons.org/licenses/by/4.0/>).

## 1. Introduction

Transition metal dichalcogenides (TMDs) have attracted a lot of attention in the past decades due to their several promising properties for electronic and optoelectronic applications. TMDs consist of a “sandwich” structure (layer) with a transition-metal sheet located in between two chalcogen sheets and possess unique properties such as energy bandgap tunable by the number of layers (from 0 to about 2.2 eV), good mobility up to few hundreds cm<sup>2</sup>V<sup>-1</sup>s<sup>-1</sup>, photoluminescence, broadband light adsorption, pristine interfaces without out-of-plane dangling bonds that allows the fabrication of hetero-structures, exceptional flexibility, thermal stability in air, and high scalability for device fabrication [1–4]. They can be produced by mechanical or liquid exfoliation, chemical vapor deposition (CVD), molecular beam epitaxy, pulsed laser deposition, etc. [5,6].

Molybdenum disulfide (MoS<sub>2</sub>) is one of the most studied transition metal dichalcogenides, owing to its layered structure and useful mechanical, chemical, electronic and optoelectronic properties [7–10]. A molybdenum (Mo) atomic plane sandwiched between two sulphur (S) planes constitutes the monolayer that is bonded to other monolayers by

weak van der Waals forces to form the bulk material. MoS<sub>2</sub> is a semiconductor suitable for several applications [11–14], having 1.2 eV indirect bandgap in the bulk form that becomes direct in the monolayer [9]. Even if it has a field-effect mobility from few tenths to hundreds [15–18] of cm<sup>2</sup>V<sup>-1</sup>s<sup>-1</sup>, lower than graphene [19,20]. MoS<sub>2</sub> field effect transistors (FETs) have recently become very popular as alternatives to graphene FETs [15–18,20–22] for next generation electronics based on 2D-materials [23–30].

MoS<sub>2</sub> nanosheets have inspired applications in pressure sensors due to their very exceptional mechanical properties. Indeed, due to the atomic thickness, the electrical properties of two-dimensional materials are highly affected by ambient gases and their pressure variations [10].

It has been reported that the adsorbed gases on the MoS<sub>2</sub> channel of FETs result in degradation of device conductance, in enhanced hysteresis and in threshold voltage shifting [10,31,32]. Conversely, vacuum annealing can increase the MoS<sub>2</sub> device conductance by desorbing the gas molecules.

The fabrication and characterization of devices based on 2D materials often rely on irradiation by charged particles, as in the electron beam (e-beam) lithography (EBL) or focussed ion beam processing as well as on scanning (SEM) or transmission electron microscopy (TEM). The exposure to low-energy electrons and/or ions can modify the electronic properties of the 2D, as structural defects can locally modify the band structure and behave as charge traps, thereby changing the device characteristics [33,34].

TMDs possess atomically sharp edges and localized defects that can enhance the local electric field and enable the extraction of a field emission (FE) current with low turn-on voltage. FE is a quantum mechanical phenomenon in which electrons, extracted from a conductor or a semiconductor surface under application of an intense electric field, move in vacuum from a cathode to an anode. FE is used in a variety of applications, ranging from electrically-operated floating-gate memory cells [35,36], electron microscopy [37] and e-beam lithography [38] to display technology or vacuum electronics [39].

Fowler and Nordheim developed a field emission theory for planar electrodes that is commonly applied also to rough surfaces where tip-shaped protrusions enhance the local electric field and emit electrons at a reduced anode-to-cathode voltage [40].

In this paper, we use CVD to fabricate monolayer MoS<sub>2</sub> flakes on a SiO<sub>2</sub>/Si substrate and characterize their transport properties. We studied their electric properties under electron beam irradiation and varying the pressure. Furthermore, using a tip anode that can be accurately positioned near the edge of the flake, we investigate the local field emission properties of MoS<sub>2</sub> nanosheets.

## 2. Materials and Methods

A three-zone split tube furnace, purged with 1000 Ncm<sup>3</sup>/min of Ar gas for 15 min to minimize the O<sub>2</sub> content, was used to grow MoS<sub>2</sub> flakes by CVD. The p-Si substrate capped by 285 nm thick SiO<sub>2</sub> was initially spin coated with 1% sodium cholate solution. The substrate and the MoO<sub>3</sub> precursor, obtained from a saturated ammonium heptamolybdate (AHM) solution annealed at 300 °C under ambient conditions, were placed in one of the three zones of the tube furnace, while 50 mg of S powder were positioned upstream in a separate heating zone. The zones containing the S and MoO<sub>3</sub> were heated to 150 °C and 750 °C, respectively. The growth process was stopped after 15 min and the sample was cooled down rapidly [41].

Larger MoS<sub>2</sub> flakes were selected to fabricate field-effect transistors (FET) through standard photolithography and lift-off processes. Figures 1a,b show the scanning electron microscope (SEM) top view of a typical device and its schematic layout and biasing circuit. The Si substrate is the back-gate while the evaporated Ti/Au (10/40 nm) electrodes are the source and the drain of the FET.

The electrical measurements were carried out inside an SEM chamber (LEO 1530, Zeiss, Oberkochen, Germany), endowed with two metallic probes (tungsten tips) connected to a Keithley 4200 Source Measurement Unit (SCS, Tektronix Inc., Beaverton, OR,

USA). Piezoelectric motors control the motion of the tips that can be positioned with nanometer precision. The chamber was usually kept at room temperature and pressure below  $10^{-6}$  Torr.

In the following, the electrical characterization refers to the transistor between the contacts labelled as 1 and 2 in Figure 1a. The contact 1 constitutes the drain and 2 the grounded source (Figure 1b).

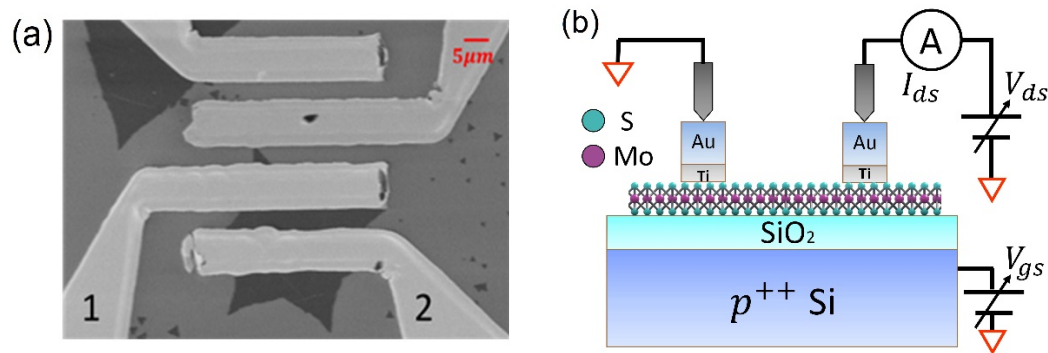


**Figure 1.** (a) Scanning electron microscope image of a typical device (top-view); (b) Schematic layout and biasing circuit.

### 3. Results and Discussion

The result of transfer characteristic measurements at different pressures,  $P$ , from high vacuum to atmospheric pressure is displayed in Figure 2a. The increasing air pressure causes a left-shift of the transfer curve and therefore an increase of transistor threshold voltage,  $V_{th}$ . The threshold voltage is here defined as the  $x$ -axis intercept of the straight lines fitting the  $I_{ds} - V_{gs}$  curves in the current range 1–100 nA. We note that the effect of air pressure on the channel conductance, which could result in the dramatic transformation of n-type to p-type conduction when passing from high vacuum to atmospheric pressure, has been reported also for other 2D TMDs materials such as  $WSe_2$  or  $PdSe_2$  (REF). The effect is usually reversible although it has been found that an aging can occur in specific TMDs, such as  $PdSe_2$ , after a long (>20 days) air exposure at atmospheric pressure [32].

The monotonic  $V_{th} - P$  behaviour, shown in Figure 3b, suggests that the transistor can be used as pressure sensor, with maximum sensitivity up to  $\frac{dV}{d(\log_{10} P)} \approx 13 \frac{V}{\text{decade}}$  at lower pressures, where the  $V_{th} - P$  curve is steeper. Besides the higher sensitivity, the duty cycle of the device increases when operated in vacuum because of the suppressed air aging effect. Therefore, the sensor is best suited as a vacuum gauge. Moreover, the sensor can be operated in low power-consumption regime as is needed a current of 1 nA or less to monitor the  $V_{th}$  variation.

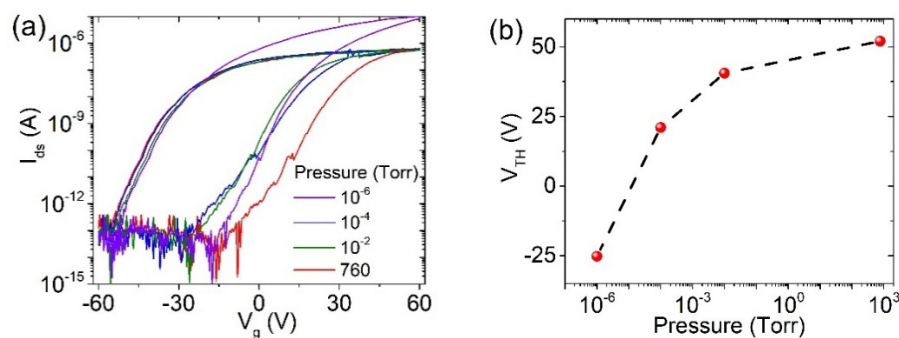


**Figure 2.** (a) Transfer characteristic of the device varying the pressure; (b) Threshold voltage right shifts decreasing the pressure.

The device contact 1 has been exposed to the SEM electron beam. Each exposure lasted 300 s corresponding to a fluence of  $\sim 180 \frac{e^-}{\text{nm}^2}$ , over a surface of  $\sim 100 \mu\text{m}^2$ . As the shape and the current intensity of the output characteristics is related to the Schottky barrier heights at the contacts, the exponentially increasing current displayed in Figure 3a induced Schottky barrier lowering. The energy release in the metal contacts can modify the chemistry of the metal/MoS<sub>2</sub> interface or create stress and defects that can lead to a lowering of the barrier and a consequent contact resistance reduction. We note that the reduction of the contact resistance by chemical reactions between the metal contacts and MoS<sub>2</sub> channel has been reported for metal deposited under ultrahigh vacuum [42] and contact laser annealing [43]. A disordered, compositionally graded layer, composed of Mo and Ti<sub>x</sub>S<sub>y</sub> species, forms at the surface of the MoS<sub>2</sub> crystal following the deposition of Ti, and thermal annealing in the 100–600 °C temperature range can cause Ti diffusion inducing further chemical and structural changes at the Ti/MoS<sub>2</sub> interface [44,45]. It is also possible that diffusion of Au atoms to the interface with MoS<sub>2</sub> occurs under the energetic electron beam irradiation. Au does not react with MoS<sub>2</sub> but reduces the contact resistance and therefore to the Schottky barrier height.

Figure 3b shows the Schottky barrier variation at the interface of the contact 1 and the flake, calculated as reported in reference [46].

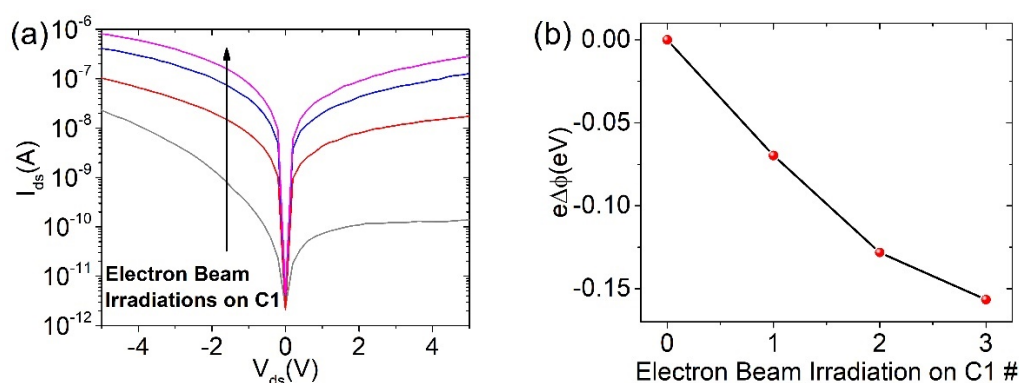


**Figure 3.** (a) Output characteristic of the device before e-beam irradiation (grey) and after 1 (red), 2 (blue) and 3 (pink) exposure to the beam. (b) Schottky barrier variation at the interface between contact 1 and the MoS<sub>2</sub> flake.

The intrinsic and gate-controllable n-type doping, the low electron affinity (4.2 eV [47]), and the nanosheets' sharp edges make 2D MoS<sub>2</sub> appealing for FE applications [8,11]. To perform field emission measurements, we used the configuration in the inset of Figure 4a.

Figure 4a shows two curves of field emission current measurements performed at  $d = 200 \text{ nm}$  anode-cathode distance. They show repeatable FE current occurring with about  $180 \text{ V}/\mu\text{m}$  turn-on field (defined as the field to which the current emerges from the noise floor).

According to the Fowler–Nordheim (FN) model, the FE current from a semiconductor can be described as [48]:

$$I_{FE} = Sa \frac{E_S^2}{\chi} e^{-b \frac{\chi^3/2}{E_S}} \quad (1)$$

where  $S$  is the emitting surface area,  $a = 1.54 \times 10^{-6} \text{ A V}^{-2} \text{ eV}$  and  $b = 6.83 \times 10^7 \text{ V cm}^{-1} \text{ eV}^{-3/2}$  are constants,  $E_S (\text{V cm}^{-1})$  is the electric field at the emitting surface and  $\chi$  is the electron affinity of the emitting material. The electric field  $E_S = \beta V / (k \cdot d)$ , with  $\beta$  the so-called field enhancement factor, i.e., the ratio between the electric field at the sample surface and the applied field  $V / (k \cdot d)$ , and  $k \sim 1.6$  a phenomenological factor accounting for the spherical shape of the tip [49,50]. The Fowler–Nordheim equation leads

to the linear behaviour of the so-called FN plot of  $\ln(I_{FE}/V^2)$  vs.  $1/V$  of Figure 4b, which allows to estimate the  $\beta$  factor as 16.5.

The back gate can be used to electrically control the doping level of the MoS<sub>2</sub> channel. Greater availability of conduction electrons increases the tunneling probability. Therefore, a positive voltage on the gate is expected to enhance the field emission current.

Indeed, Figure 4c confirms an increasing field emission current for increasing gate voltages.

The data of Figure 4c provide the proof-of-concept of a new MoS<sub>2</sub> field-effect transistor based on field emission. The transfer characteristic of the device, at different anode voltages  $V$ , are shown in Figure 4d. The exponential growth of the field emission current for increasing  $V_{gs}$  is well explained in reference [51].

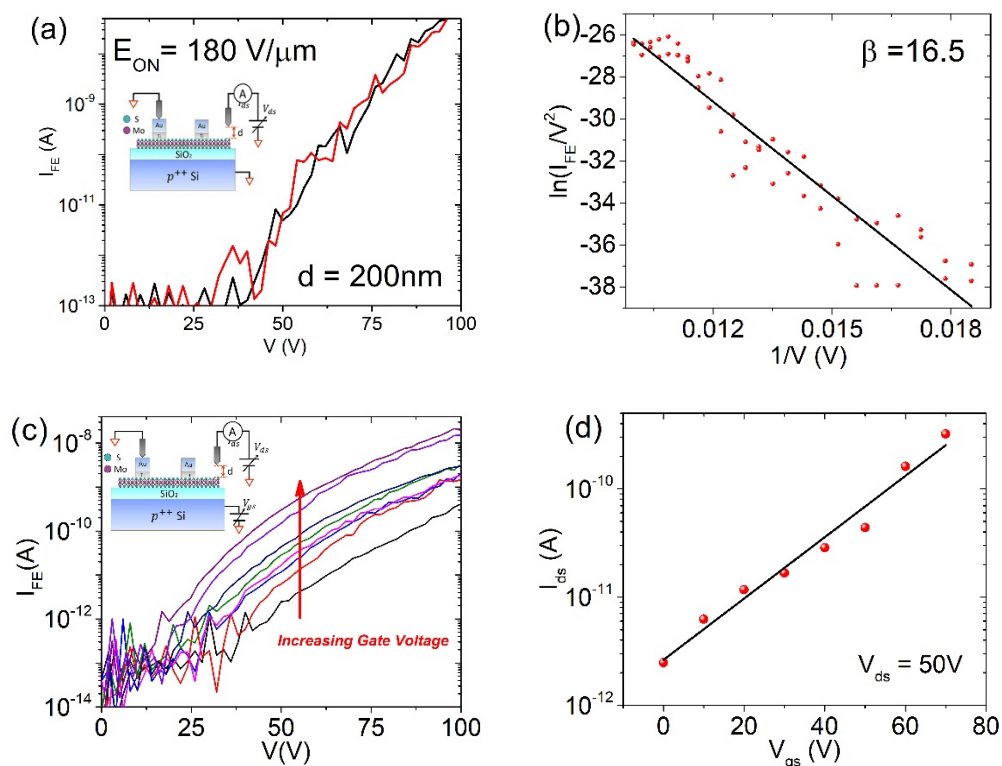


**Figure 4.** (a) Field emission current measured using the schematic in the inset; (b) Fowler-Nordheim analysis resulting in a beta factor of 16.5; (c) Field emission measurements varying the applied voltage on the back-gate, as in the inset; (d) Transfer characteristic of this field-effect transistor based on field emission.

#### 4. Conclusions

We have fabricated and electrically characterized monolayer MoS<sub>2</sub> field effect transistors. We have found that the threshold voltage of the transistor increases monotonously with the air pressure. We investigated the effects of 10 keV electron beam irradiation of the Schottky metal contacts in MoS<sub>2</sub> based FETs. The electrical measurements revealed that electron beam irradiation improves the device conductance, reduces the rectification of the output characteristic and causes a left-shift of the threshold voltage. A field emission current, following the FN model, has been measured from the edge of the MoS<sub>2</sub> nanosheets. More importantly, it has been shown that the gate voltage can modulate the FE current thus featuring a new transistor based on field emission. This finding constitutes a first step toward a device with great application potential, especially if implemented with the current flowing parallel to the substrate surface.

**Institutional Review Board Statement:** Not applicable.

**Informed Consent Statement:** Not applicable.

**Data Availability Statement:** The data presented in this study are available on request from the corresponding author.

## References

1. Gupta, A.; Sakthivel, T.; Seal, S. Recent development in 2D materials beyond graphene. *Prog. Mater. Sci.* **2015**, *73*, 44–126, doi:10.1016/j.pmatsci.2015.02.002.
2. Choi, W.; Choudhary, N.; Han, G.H.; Park, J.; Akinwande, D.; Lee, Y.H. Recent development of two-dimensional transition metal dichalcogenides and their applications. *Mater. Today* **2017**, *20*, 116–130, doi:10.1016/j.mattod.2016.10.002.
3. Di Bartolomeo, A. Emerging 2D Materials and Their Van Der Waals Heterostructures. *Nanomaterials* **2020**, *10*, 579, doi:10.3390/nano10030579.
4. Jariwala, D.; Sangwan, V.K.; Lauhon, L.J.; Marks, T.J.; Hersam, M.C. Emerging Device Applications for Semiconducting Two-Dimensional Transition Metal Dichalcogenides. *ACS Nano* **2014**, *8*, 1102–1120, doi:10.1021/nr500064s.
5. Huang, J.; Yang, L.; Liu, D.; Chen, J.; Fu, Q.; Xiong, Y.; Lin, F.; Xiang, B. Large-area synthesis of monolayer WSe<sub>2</sub> on a SiO<sub>2</sub>/Si substrate and its device applications. *Nanoscale* **2015**, *7*, 4193–4198, doi:10.1039/C4NR07045C.
6. Jawaid, A.; Nepal, D.; Park, K.; Jespersen, M.; Qualley, A.; Mirau, P.; Drummy, L.F.; Vaia, R.A. Mechanism for Liquid Phase Exfoliation of MoS<sub>2</sub>. *Chem. Mater.* **2016**, *28*, 337–348, doi:10.1021/acs.chemmater.5b04224.
7. Santhosh, S.; Madhavan, A.A. A review on the structure, properties and characterization of 2D Molybdenum Disulfide. In Proceedings of the 2019 Advances in Science and Engineering Technology International Conferences (ASET), Dubai, UAE, 26 March–10 April 2019; IEEE: Dubai, UAE, 2019; pp. 1–5.
8. Urban, F.; Passacantando, M.; Giubileo, F.; Iemmo, L.; Di Bartolomeo, A. Transport and Field Emission Properties of MoS<sub>2</sub> Bilayers. *Nanomaterials* **2018**, *8*, 151, doi:10.3390/nano8030151.
9. Mak, K.F.; Lee, C.; Hone, J.; Shan, J.; Heinz, T.F. Atomically Thin MoS<sub>2</sub>: A New Direct-Gap Semiconductor. *Phys. Rev. Lett.* **2010**, *105*, 136805, doi:10.1103/PhysRevLett.105.136805.
10. Urban, F.; Giubileo, F.; Grillo, A.; Iemmo, L.; Luongo, G.; Passacantando, M.; Foller, T.; Madauß, L.; Pollmann, E.; Geller, M.P.; et al. Gas dependent hysteresis in MoS<sub>2</sub> field effect transistors. *2D Mater.* **2019**, *6*, 045049, doi:10.1088/2053-1583/ab4020.
11. Giubileo, F.; Grillo, A.; Passacantando, M.; Urban, F.; Iemmo, L.; Luongo, G.; Pelella, A.; Loveridge, M.; Lozzi, L.; Di Bartolomeo, A. Field Emission Characterization of MoS<sub>2</sub> Nanoflowers. *Nanomaterials* **2019**, *9*, 717, doi:10.3390/nano9050717.
12. Hasani, A.; Le, Q.V.; Tekalgne, M.; Choi, M.-J.; Lee, T.H.; Jang, H.W.; Kim, S.Y. Direct synthesis of two-dimensional MoS<sub>2</sub> on p-type Si and application to solar hydrogen production. *Npg Asia Mater* **2019**, *11*, 47, doi:10.1038/s41427-019-0145-7.
13. Dragoman, M.; Cismaru, A.; Aldrigo, M.; Radoi, A.; Dinescu, A.; Dragoman, D. MoS<sub>2</sub> thin films as electrically tunable materials for microwave applications. *Appl. Phys. Lett.* **2015**, *107*, 243109, doi:10.1063/1.4938145.
14. Madauß, L.; Zegkinoglou, I.; Vázquez Muiños, H.; Choi, Y.-W.; Kunze, S.; Zhao, M.-Q.; Naylor, C.H.; Ernst, P.; Pollmann, E.; Ochedowski, O.; et al. Highly active single-layer MoS<sub>2</sub> catalysts synthesized by swift heavy ion irradiation. *Nanoscale* **2018**, *10*, 22908–22916, doi:10.1039/C8NR04696D.
15. Di Bartolomeo, A.; Santandrea, S.; Giubileo, F.; Romeo, F.; Petrosino, M.; Citro, R.; Barbara, P.; Lupina, G.; Schroeder, T.; Rubino, A. Effect of back-gate on contact resistance and on channel conductance in graphene-based field-effect transistors. *Diam. Relat. Mater.* **2013**, *38*, 19–23, doi:10.1016/j.diamond.2013.06.002.
16. Wilmart, Q.; Boukhicha, M.; Graef, H.; Mele, D.; Palomo, J.; Rosticher, M.; Taniguchi, T.; Watanabe, K.; Bouchiat, V.; Baudin, E.; et al. High-Frequency Limits of Graphene Field-Effect Transistors with Velocity Saturation. *Appl. Sci.* **2020**, *10*, 446, doi:10.3390/app10020446.
17. Piccinini, E.; Alberti, S.; Longo, G.S.; Berninger, T.; Breu, J.; Dostalek, J.; Azzaroni, O.; Knoll, W. Pushing the Boundaries of Interfacial Sensitivity in Graphene FET Sensors: Polyelectrolyte Multilayers Strongly Increase the Debye Screening Length. *J. Phys. Chem. C* **2018**, *122*, 10181–10188, doi:10.1021/acs.jpcc.7b11128.
18. Di Bartolomeo, A.; Giubileo, F.; Iemmo, L.; Romeo, F.; Russo, S.; Unal, S.; Passacantando, M.; Grossi, V.; Cucolo, A.M. Leakage and field emission in side-gate graphene field effect transistors. *Appl. Phys. Lett.* **2016**, *109*, 023510, doi:10.1063/1.4958618.
19. Urban, F.; Lupina, G.; Grillo, A.; Martucciello, N.; Di Bartolomeo, A. Contact resistance and mobility in back-gate graphene transistors. *Nano Express* **2020**, *1*, 010001, doi:10.1088/2632-959X/ab7055.
20. Bolotin, K.I. Electronic transport in graphene: Towards high mobility. In *Graphene*; Elsevier: Amsterdam, The Netherlands, 2014; pp. 199–227. ISBN 978-0-85709-508-4.
21. Bartolomeo, A.D.; Giubileo, F.; Romeo, F.; Sabatino, P.; Carapella, G.; Iemmo, L.; Schroeder, T.; Lupina, G. Graphene field effect transistors with niobium contacts and asymmetric transfer characteristics. *Nanotechnology* **2015**, *26*, 475202, doi:10.1088/0957-4484/26/47/475202.
22. Li, F.; Gao, F.; Xu, M.; Liu, X.; Zhang, X.; Wu, H.; Qi, J. Tuning Transport and Photoelectric Performance of Monolayer MoS<sub>2</sub> Device by E-Beam Irradiation. *Adv. Mater. Interfaces* **2018**, *5*, 1800348, doi:10.1002/admi.201800348.
23. Wang, J.; Yao, Q.; Huang, C.-W.; Zou, X.; Liao, L.; Chen, S.; Fan, Z.; Zhang, K.; Wu, W.; Xiao, X.; et al. High Mobility MoS<sub>2</sub> Transistor with Low Schottky Barrier Contact by Using Atomic Thick h-BN as a Tunneling Layer. *Adv. Mater.* **2016**, *28*, 8302–8308, doi:10.1002/adma.201602757.

24. Fiori, G.; Bonaccorso, F.; Iannaccone, G.; Palacios, T.; Neumaier, D.; Seabaugh, A.; Banerjee, S.K.; Colombo, L. Electronics based on two-dimensional materials. *Nat. Nanotech* **2014**, *9*, 768–779, doi:10.1038/nnano.2014.207.
25. Kim, M.J.; Choi, Y.; Seok, J.; Lee, S.; Kim, Y.J.; Lee, J.Y.; Cho, J.H. Defect-Free Copolymer Gate Dielectrics for Gating MoS<sub>2</sub> Transistors. *J. Phys. Chem. C* **2018**, *122*, 12193–12199, doi:10.1021/acs.jpcc.8b03092.
26. Di Bartolomeo, A.; Pelella, A.; Liu, X.; Miao, F.; Passacantando, M.; Giubileo, F.; Grillo, A.; Iemmo, L.; Urban, F.; Liang, S. Pressure-Tunable Ambipolar Conduction and Hysteresis in Thin Palladium Diselenide Field Effect Transistors. *Adv. Funct. Mater.* **2019**, *29*, 1902483, doi:10.1002/adfm.201902483.
27. Di Bartolomeo, A.; Luongo, G.; Iemmo, L.; Urban, F.; Giubileo, F. Graphene–Silicon Schottky Diodes for Photodetection. *IEEE Trans. Nanotechnol.* **2018**, *17*, 1133–1137, doi:10.1109/TNANO.2018.2853798.
28. Jin, C.; Rasmussen, F.A.; Thygesen, K.S. Tuning the Schottky Barrier at the Graphene/MoS<sub>2</sub> Interface by Electron Doping: Density Functional Theory and Many-Body Calculations. *J. Phys. Chem. C* **2015**, *119*, 19928–19933, doi:10.1021/acs.jpcc.5b05580.
29. Grillo, A.; Di Bartolomeo, A.; Urban, F.; Passacantando, M.; Caridad, J.M.; Sun, J.; Camilli, L. Observation of 2D Conduction in Ultrathin Germanium Arsenide Field-Effect Transistors. *ACS Appl. Mater. Interfaces* **2020**, *12*, 12998–13004, doi:10.1021/acsami.0c00348.
30. Di Bartolomeo, A.; Genovese, L.; Giubileo, F.; Iemmo, L.; Luongo, G.; Foller, T.; Schleberger, M. Hysteresis in the transfer characteristics of MoS<sub>2</sub> transistors. *2D Mater.* **2017**, *5*, 015014, doi:10.1088/2053-1583/aa91a7.
31. Hoffman, A.N.; Gu, Y.; Liang, L.; Fowlkes, J.D.; Xiao, K.; Rack, P.D. Exploring the air stability of PdSe<sub>2</sub> via electrical transport measurements and defect calculations. *npj 2D Mater. Appl.* **2019**, *3*, 50, doi:10.1038/s41699-019-0132-4.
32. Giubileo, F.; Iemmo, L.; Passacantando, M.; Urban, F.; Luongo, G.; Sun, L.; Amato, G.; Enrico, E.; Di Bartolomeo, A. Effect of Electron Irradiation on the Transport and Field Emission Properties of Few-Layer MoS<sub>2</sub> Field-Effect Transistors. *J. Phys. Chem. C* **2019**, *123*, 1454–1461, doi:10.1021/acs.jpcc.8b09089.
33. Di Bartolomeo, A.; Urban, F.; Pelella, A.; Grillo, A.; Passacantando, M.; Liu, X.; Giubileo, F. Electron irradiation of multilayer PdSe<sub>2</sub> field effect transistors. *Nanotechnology* **2020**, *31*, 375204, doi:10.1088/1361-6528/ab9472.
34. Aplin, K.L.; Kent, B.J.; Wang, L.; Lockwood, H.F.; Rouse, J.; Stevens, R. Variability in long-duration operation of silicon tip field emission devices. *J. Vac. Sci. Technol. B* **2006**, *24*, 1056, doi:10.1116/1.2177229.
35. Di Bartolomeo, A.; Yang, Y.; Rinzan, M.B.M.; Boyd, A.K.; Barbara, P. Record Endurance for Single-Walled Carbon Nanotube–Based Memory Cell. *Nanoscale Res. Lett.* **2010**, *5*, 1852–1855, doi:10.1007/s11671-010-9727-6.
36. Li, Y.; Sun, Y.; Jaffray, D.A.; Yeow, J.T.W. Coulomb explosion of vertically aligned carbon nanofibre induced by field electron emission. *RSC Adv.* **2017**, *7*, 40470–40479, doi:10.1039/C7RA07474C.
37. Wieland, M.J.; Kampherbeek, B.J.; Addressi, P.; Kruit, P. Field emission photocathode array for multibeam electron lithography. *Microelectron. Eng.* **2001**, *57–58*, 155–161, doi:10.1016/S0167-9317(01)00507-X.
38. Furse, G.N. Field emission in vacuum micro-electronics. *Appl. Surf. Sci.* **2003**, *215*, 113–134, doi:10.1016/S0169-4332(03)00315-5.
39. Fowler-Nordheim equation. In *Introduction to the Physics of Electron Emission*; John Wiley & Sons, Ltd.: Chichester, UK, 2017; pp. 139–148. ISBN 978-1-119-05179-4.
40. Pollmann, E.; Madauß, L.; Schumacher, S.; Kumar, U.; Heuvel, F.; Ende, C. vom; Yilmaz, S.; Gündörmüs, S.; Schleberger, M. Apparent Differences between Single Layer Molybdenum Disulfide Fabricated via Chemical Vapor Deposition and Exfoliation. *arXiv* **2020**, arXiv:2006.05789.
41. Smyth, C.M.; Addou, R.; McDonnell, S.; Hinkle, C.L.; Wallace, R.M. Contact Metal–MoS<sub>2</sub> Interfacial Reactions and Potential Implications on MoS<sub>2</sub>–Based Device Performance. *J. Phys. Chem. C* **2016**, *120*, 14719–14729, doi:10.1021/acs.jpcc.6b04473.
42. Kwon, H.; Baik, S.; Jang, J.; Kim, S.; Grigoropoulos, C.; Kwon, H.-J. Ultra-Short Pulsed Laser Annealing Effects on MoS<sub>2</sub> Transistors with Asymmetric and Symmetric Contacts. *Electronics* **2019**, *8*, 222, doi:10.3390/electronics8020222.
43. McDonnell, S.; Smyth, C.; Hinkle, C.L.; Wallace, R.M. MoS<sub>2</sub>–Titanium Contact Interface Reactions. *ACS Appl. Mater. Interfaces* **2016**, *8*, 8289–8294, doi:10.1021/acsami.6b00275.
44. Freedy, K.M.; Zhang, H.; Litwin, P.M.; Bendersky, L.A.; Davydov, A.V.; McDonnell, S. Thermal Stability of Titanium Contacts to MoS<sub>2</sub>. *ACS Appl. Mater. Interfaces* **2019**, *11*, 35389–35393, doi:10.1021/acsami.9b08829.
45. Pelella, A.; Kharsah, O.; Grillo, A.; Urban, F.; Passacantando, M.; Giubileo, F.; Iemmo, L.; Sleziona, S.; Pollmann, E.; Madauß, L.; et al. Electron irradiation of metal contacts in monolayer MoS<sub>2</sub> Field-Effect Transistors. *arXiv* **2020**, arXiv:2004.00903.
46. Sup Choi, M.; Lee, G.-H.; Yu, Y.-J.; Lee, D.-Y.; Hwan Lee, S.; Kim, P.; Hone, J.; Jong Yoo, W. Controlled charge trapping by molybdenum disulphide and graphene in ultrathin heterostructured memory devices. *Nat. Commun.* **2013**, *4*, 1624, doi:10.1038/ncomms2652.
47. Jensen, K.L. Electron emission theory and its application: Fowler–Nordheim equation and beyond. *J. Vac. Sci. Technol. B* **2003**, *21*, 1528, doi:10.1116/1.1573664.
48. Di Bartolomeo, A.; Scarfato, A.; Giubileo, F.; Bobba, F.; Biasiucci, M.; Cucolo, A.M.; Santucci, S.; Passacantando, M. A local field emission study of partially aligned carbon-nanotubes by atomic force microscope probe. *Carbon* **2007**, *45*, 2957–2971, doi:10.1016/j.carbon.2007.09.049.
49. Sun, S.; Ang, L.K. Analysis of nonuniform field emission from a Lorentzian or Hyperboloid shape emitter. In Proceedings of the 2013 Abstracts IEEE International Conference on Plasma Science (ICOPS), San Francisco, CA, USA, 2013; IEEE: San Francisco, CA, USA, 2013; p. 1.
50. Pelella, A.; Grillo, A.; Urban, F.; Giubileo, F.; Passacantando, M.; Pollmann, E.; Sleziona, S.; Schleberger, M.; Di Bartolomeo, A. Gate-controlled field emission current from MoS<sub>2</sub> nanosheets. *arXiv* **2020**, arXiv:2008.09910.